

Pruning at Initialization - A Sketching Perspective

Noga Bar
Tel Aviv University
Tel Aviv, Israel
nogabar@mail.tau.ac.il

Raja Giryes
Tel Aviv University
Tel Aviv, Israel
raja@tauex.tau.ac.il

Abstract

The lottery ticket hypothesis (LTH) has increased attention to pruning neural networks at initialization. We study this problem in the linear setting. We show that finding a sparse mask at initialization is equivalent to the sketching problem introduced for efficient matrix multiplication. This gives us tools to analyze the LTH problem and gain insights into it. Specifically, using the mask found at initialization, we bound the approximation error of the pruned linear model at the end of training. We theoretically justify previous empirical evidence that the search for sparse networks may be data independent. By using the sketching perspective, we suggest a generic improvement to existing algorithms for pruning at initialization, which we show to be beneficial in the data-independent case.

1 Introduction

Pruning a neural network at initialization, where weights are removed ahead of training, with minimal harm to network performance can be beneficial for training efficiency. It can also be used to gain insights into neural network training and expressivity as a whole. According to the lottery ticket hypothesis (LTH) [23], a network may contain extremely sparse subnetworks at initialization that achieve comparable or even better performance when trained in isolation. The original algorithm suggested for finding the winning ticket was inefficient and required multiple trainings until convergence. Others, however, suggested pruning at initialization in a more efficient manner [39, 61, 63, 17, 2, 38].

Most works propose scoring functions for finding a subnetwork at initialization that rely on the specific data and task at hand [39, 63, 17, 2]. Yet, evidence suggests that the winning lottery ticket is independent of data. Specifically, it has been shown that the winning ticket can be transferred between datasets and tasks [19, 47, 13, 57]. Moreover, previous work has shown that pruning methods can have good performance with corrupted training data [60]. Furthermore, the work of SynFlow has demonstrated that a network can even be pruned at initialization without the use of data and a task-specific loss [61].

In this work, we aim at explaining the success of LTH in the unsupervised setting without data. Previous theoretical analysis focused on a stronger version of the LTH [56]. According to the study, deep neural networks have a sparse subnetwork capable of good performance even without training in a supervised setting. Specifically, they show that for a given deep neural network (DNN) architecture, initialization and target data (with labels), there is a subnetwork that achieves high accuracy without the need to train. The theoretical explanation for the strong LTH is developed by estimating the function produced by the large and dense network using only the sparse subnetworks in it [43, 55]. This result was further generalized and it has been shown that the initialization can be compatible with a set of functions over the training set [10]. While the above results provide an intriguing explanation for the success of LTH in the supervised case, their explanation for the existence of the mask assumes the data is available for performing the pruning and that no training is required. Our

study, on the other hand, focuses on the unsupervised setting, where pruning is performed using random data and applied to other parameters than the ones at initialization (possibly after training).

For our analysis, we draw a connection between pruning at initialization and a well known sketching algorithm [18]. Originally, the algorithm was suggested for efficient matrix multiplication while minimizing the error of the multiplication approximation. We choose to focus on the linear case and analyse it in order to gain insights into the general case, which is a common practice when analyzing neural networks [4, 9, 58, 5, 40, 3, 50, 68].

The key observation in our work is that in the linear case, the sketching algorithm corresponds to the pruning at initialization problem. Based on this relationship, we extend the sketching analysis of the approximation error at initialization for the case of an unknown vector. In our case, this vector can be interpreted as the learned vector at the end of training. We focus on the correspondence between sketching and pruning without data. This allows us to analyze the performance of pruning algorithms that operates in the unsupervised regime, i.e., without labeled training data. We develop a bound that shows that the error in pruning without data depends on the distance between the weights of the linear network at initialization and at the end of training.

This distance is known to be small in practical NNs and especially in the Neural Tangent Kernel (NTK) regime [37, 32, 6], where the network width grows to infinity. Under common assumptions in NTK settings, we consider network output features as linear random features. Based on these assumptions, we prove that the mask found by sketching also approximates the network output features.

Equipped with the theoretical results, we turn to study practical algorithms for the problem of pruning at initialization without data. We consider the state-of-the-art and unsupervised SynFlow method and show that in the linear case it bears great similarity to sketching when is applied with a random vector. This provides us with a possible explanation for SynFlow’s success. We also analyse the connection of the supervised SNIP method to sketching and use it to suggest an unsupervised version of SNIP.

The relations we draw also suggest that successful pruning is highly correlated with selecting weights that have large magnitude at initialization. We empirically validate our findings for both SynFlow and the iterative magnitude pruning (IMP) algorithm (the method suggested in the original LTH work) showing that they both have the tendency to maintain large magnitude weights after pruning.

To further validate our analysis with random data, we show that for various known pruning algorithms that make use of the input data [23, 63, 39] that their performance only mildly degrades when the input is replaced with completely random input. This stands in line with previous evidence that pruning methods do not exploit the data [60].

Based on the above results, we suggest a general improvement to existing pruning algorithms in the unsupervised case. Instead of pruning weights by removing the lowest scores, sketching masks are randomized based on some probability. We test the effect of replacing the strict threshold criterion of pruning with a randomized one in which the mask is sampled based on the pruning method scoring. This strategy shows improvement in most cases for various network architectures and datasets, namely, CIFAR-10, CIFAR-100 [35] and Tiny-ImageNet [66].

2 Related Work

The main research approach for pruning deep neural networks follows the train→prune→fine-tune pipeline [49, 46, 36, 29, 28, 27]. Those methods require training until convergence, then pruning and finally fine tuning. Thus, they have the ability to save computations at inference time. Another approach for pruning is sparsifying the model during training where training and pruning are performed simultaneously [12, 11, 42, 8, 45, 48, and more]. In this case, the fine tuning stage is omitted. Those methods have limited ability to improve training efficiency and the gain is mainly for inference time. Lastly, pruning at initialization, which is our focus, aims to zero parameters at initialization. Such methods can improve efficiency in parameters for both training and inference [19]. Additionally, it can be used for neural architecture search [44, 64, 1] and for gaining a deeper theoretical understanding of DNN [7].

In this work, we discuss pruning network by simply zeroing weights (unstructured pruning). Yet, another approach is to remove complete neurons of the network (structured pruning) [52, 33, 15, 14] (for a comprehensive survey see [51]). These methods generally include more parameters than unstructured ones but are usually more beneficial for computational time on standard hardware. However, unstructured pruned models also have this advantages as it can lead to reduced computations for some hardware while maintaining a low number of parameters [19]. In addition, a method originally presented for unstructured pruning that employs scoring has been extended for structured pruning at initialization [62]. Therefore, the concepts presented in this work can potentially be extended to structured pruning as well.

Due to the exponential search space, pruning DNNs at initialization is a challenging task. Before LTH, it was suggested to use SNIP which prunes the NN while maintaining its connectivity according to the magnitude of the gradient [39]. SNIP has been improved by using it iteratively [17] or by applying it after a few training steps [2]. It was proposed to improve the signal propagation in the DNN at initialization [38] and to find a mask while preserving gradient flow using the Hessian matrix [63]. A sparse pruning algorithm for high-dimensional manifolds is included in [70], as well as a theoretical validation of subnetworks’ viability. Those methods rely on the gradient of their parameters w.r.t. the input data. Yet, a study found that some of these hardly exploit information from the training data [60] hinting that it may not be required for finding good sparse subnetworks. Another work, relaxed the need for supervision and employed a teacher-student model with unlabeled data [41].

The lottery ticket hypothesis (LTH) [23] has led to an increased interest in sparse neural networks. The original study suggested an exhaustive and supervised algorithm for finding the winning ticket. There are works which reduce the dependency on data when searching for the winning ticket. It was demonstrated that looking for tickets at early stages of training, prior to convergence, leads to improved performance and saves computational overhead [67, 31, 24]. It was further shown that training the LT with partial datasets leads to decent winning tickets [71]. Early pruning has been theoretically proven to be beneficial [65]. Together with other pruning methods at initialization, it was shown that the winning tickets do not rely heavily on training data [60].

Other works demonstrated the generality of the winning ticket and showed that a single pruned network can be transferred across datasets and achieve good performance after fine-tuning [19, 47, 13] and even that LT can be used for non-natural datasets [57]. The existence of universal winning tickets that fit multiple functions was shown theoretically in [10]. LTH was strengthened and it was suggested that a sparse subnetwork within the neural network initialization has high accuracy without training [56]. The strong LTH was later theoretically studied [43, 55, 53, 20, 21]. Note that strong LTH requires a larger network before pruning. This was relaxed by initializing the weights iteratively [16]. These works only bound the approximation error at initialization and assume labeled data.

SynFlow [61], a prominent method proposed for pruning at initialization, and is not data or task dependent. We examine in our study its equivalence to a sketching method when the input data to SynFlow is random rather than a vector of all ones. Additionally, other research on SynFlow proposed to examine active paths in networks at initialization [54, 25] and established data independent pruning methods. They formulate their method according to paths in the neural tangent kernel.

We establish equivalence between the sketching problem and pruning. To this end, we use a well known Monte-Carlo technique for efficient approximation of matrix multiplication and compression designed for handling large matrices [18]. We analyze network pruning methods through the ‘sketching lens’, which leads to an approximation error bound of the mask at initialization. The type of result is similar to the bounds of approximation for the strong LTH but using a different proof technique that analyze the unsupervised and “weak” case.

3 Sketching and Pruning at Initialization

Notations. The input data we aim to model is $x_i \in \mathbb{R}^d$ for $i = 1, \dots, n$ and respectively each example has its label $y_i \in \mathbb{R}$. We relate to the input as a matrix $X \in \mathbb{R}^{d \times n}$ where x_i are its columns and

$y \in \mathbb{R}^n$ is the vector containing the labels. The i th row in a matrix A is denoted as $A_{(i)}$ and the i th column as $A^{(i)}$. Unless otherwise stated, $\|x\|$ is the Euclidean norm of x .

Problem statement. In this work, we relate to linear features where we aim to find vector that approximate the data, i.e. w such that $X^T w \simeq y$. Our main interest is to sparsify w while minimizing the mean squared error of the features. The optimization problem can be written as

$$\min_{m, s.t. \|m\|_0 \leq s} \|X^T w - X^T(w \odot m)\|, \quad (1)$$

where $\|\cdot\|_0$ is the number of non-zeros in m and \odot stands for entry-wise multiplication. Clearly, when the mask is applied to a vector, it holds that $\|w \odot m\|_0 \leq s$.

Connection of sketching and pruning at initialization. We focus on a sketching approach presented initially for efficient matrix multiplication [18]. The goal in it is multiplying only a small subset of columns and rows, while harming the approximation accuracy as little as possible. The main contribution of the approach is in the way this subset is chosen. We adapt it to match the linear features settings, where the matrix multiplication is reduced to be a multiplication of given input $X \in \mathbb{R}^{d \times n}$ and a vector $w \in \mathbb{R}^d$. This results in the linear features $X^T w$.

Note that choosing rows/columns in matrix multiplication is equivalent to choosing a mask for entries in w for matrix-vector multiplication. Given a choice of the entries, the entries that are compatible with the mask are non-zero while others are zero. The zero entries in m leads to ignoring whole columns in the matrix. For example, the approximation of the multiplication of a matrix A with the vector b masked with m satisfies $Ab \simeq A(b \odot m) = A_{(\{i, m_i \neq 0\})} b_{(\{i, m_i \neq 0\})}$. This means that any sketching algorithm that compresses matrix multiplication by selecting rows/columns can also be used as a masking procedure for a vector in matrix-vector multiplication.

Algorithm 1 Sketching for mask [18].

Input: Probability $p \in \mathbb{R}^d$ and density $s \in \mathbb{Z}^+$.

Initialization Set mask $m = 0$.

for $t = 1, \dots, s$ **do**

$i_t \sim p$

$m_{i_t} = m_{i_t} + \frac{1}{sp_{i_t}}$

end for

Output: The mask m .

In order to find a mask m for the vector w as described in the problem statement (Equation (1)), we use the sketching algorithm presented in Algorithm 1. The algorithm samples an entry randomly according to the distribution p and sets this entry to be non-zero until the desired density is achieved. Note that the indices i_t are sampled i.i.d. with return and that the distribution of p is used both for sampling and scaling. Due to the possibility of sampling the same entry more than once, the resulting m has granularity of $\|m\|_0 \leq s$ and it is not necessarily holds that $\|m\|_0 = s$. Additionally, not all non-zero entries in the mask are equal.

By [18, Lemma 4] (restated in Lemma 4.1), the optimal probability for minimizing the error is

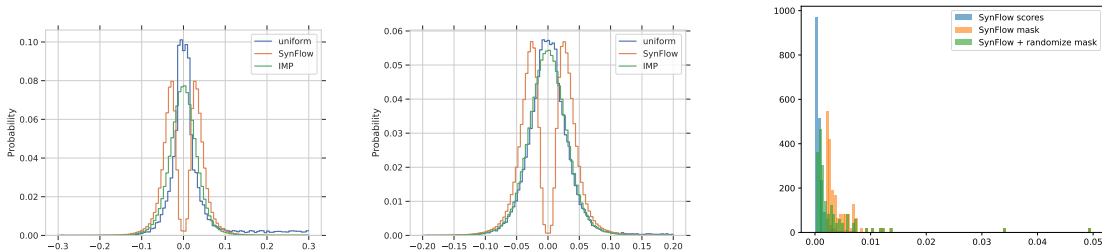
$$\Pr_{w, X}[i] = \frac{\|X_{(i)}\| |w_i|}{\sum_{j=1}^d \|X_{(j)}\| |w_j|}, \quad i = 1, \dots, d. \quad (2)$$

The probability is proportional to the norms of the rows of X , and it corresponds to a specific entry at each example x_k across all inputs, $k = 1, \dots, n$. Recall that $X_{(i)} \in \mathbb{R}^n$. Thus, masking an entry i in w means ignoring all the i th entries in the data x_k , $k = 1, \dots, n$. Note that when sampling with (2) it is more likely to choose weights with larger magnitudes given the data. Figures 1a and 2 show empirically that DNNs' pruning methods also tend to keep higher magnitude weights.

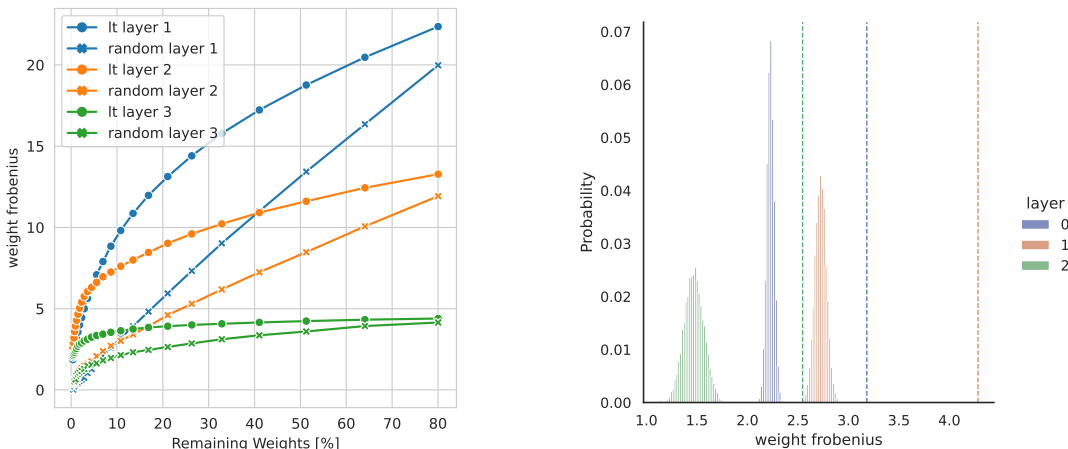
4 Pruning Approximation Error

Using the relationship between pruning and sketching drawn in Section 3, we can use the analysis tools from sketching for examining the properties of pruning. All proofs are in the Appendix B.

In pruning at initialization, the initial vector w_0 is used for finding the mask, and then we approximate the features with the same mask and another unknown vector w^* . Typically, w^* is the learned weights at the end of training. The features are $X^T w^*$ and we aim to minimize $\|X^T w^* - X^T(w^* \odot m)\|$. Note that since m is chosen randomly we bound the expected value of the approximation error. For simplicity, we use the notation of $p_i^0 = \Pr_{w^0, X}[i]$ as detailed in Equation (2). p^0 is the optimal



(a) Weights histogram in sparse subnetworks at initialization for VGG-19 and CIFAR-10. Note that SynFlow and IMP have bias to large magnitude weights compared to a uniformly random mask. (b) Histogram of scores of NN before pruning and the weights chosen by SynFlow w./w.o. randomization.



(a) Norms of winning lottery tickets and random masks with multiple sparsities. (b) Norms of winning lottery tickets compared to 10,000 random masks with 1.2% density.

Figure 2: Winning tickets norms vs. random tickets with Fashion-MNIST and a fully connected NN.

probability to sample the mask at initialization. In our analysis, X may be given or randomly distributed while the weighting w is assumed to be known.

First, we present a simplified version of the one found in the original sketching paper [18] assuming the data X are given. We rephrase the lemma to match the vector-matrix multiplication case.

Lemma 4.1. [Simplified version of [18, Lemma 4]] Suppose $X \in \mathbb{R}^{d \times n}$, $w^0 \in \mathbb{R}^d$ and $s \in \mathbb{Z}^+$ then using Algorithm 1 with p^0 for m then the error is

$$\mathbb{E}_{m|X} \left[\|X^T w^0 - X^T (w^0 \odot m)\|^2 \right] = \frac{1}{s} \left(\sum_{k=1}^d \|X_{(k)}\| |w_k^0| \right)^2 - \frac{1}{s} \|X^T w^0\|^2$$

The lemma bounds the error of sparse approximation at initialization when the data is given. It is proportional to $\frac{1}{s}$, which means that as the density of the mask grows the error decreases, as expected. This connection will be consistent throughout our analysis. Next, we establish a bound of the error when X is drawn from a normal i.i.d. distribution, where we also observe this behavior.

Lemma 4.2. Suppose $X \in \mathbb{R}^{d \times n} \sim \frac{1}{\sqrt{n}} \mathcal{N}(0, I)$, $w^0 \in \mathbb{R}^d$ and $s \in \mathbb{Z}^+$ then when using Algorithm 1 with p^0 for drawing m , the error can be bounded as follows

$$\mathbb{E}_X \left[\|X^T w^0 - X^T (w^0 \odot m)\|^2 \right] \leq \frac{1}{s} \|w^0\|^2.$$

Note that the above error bounds holds at initialization. Yet, in the pruning at initialization setting, unlike matrix multiplication, we do not aim to apply a mask on a known parameter w^0 but on some

Table 1: Accuracy results for vanilla SynFlow [61], SynFlow with χ distributed input and with mask randomization; and accuracy results for SNIP [39] with normal random data, sparse input data and mask randomization. Above are results with CIFAR-10 and below are results with CIFAR-100.

Model	Density	SynFlow	SynFlow + χ	SynFlow + rand. mask	SynFlow + rand. mask + χ	SNIP + normal data	SNIP + rand. mask + normal. data	SNIP + sparse data	SNIP + sparse data + rand. mask
VGG-19	10%	93.01 \pm 0.19	93.12 \pm 0.12	93.06 \pm 0.12	93.12 \pm 0.18	92.15 \pm 0.07	92.55 \pm 0.57	92.85 \pm 0.06	93.16 \pm 0.36
	5%	92.68 \pm 0.11	92.52 \pm 0.20	92.44 \pm 0.11	92.63 \pm 0.2	91.53 \pm 0.04	92.18 \pm 0.78	92.02 \pm 0.18	92.79 \pm 0.78
	2%	91.68 \pm 0.28	91.32 \pm 0.11	91.63 \pm 0.16	91.71 \pm 0.28	90.35 \pm 0.31	91.04 \pm 0.14	90.97 \pm 0.11	92.03 \pm 0.91
ResNet-20	10%	86.55 \pm 0.18	86.70 \pm 0.32	86.74 \pm 0.22	86.59 \pm 0.29	85.69 \pm 0.37	86.77 \pm 0.41	85.85 \pm 0.07	87.02 \pm 0.65
	5%	83.19 \pm 0.36	83.28 \pm 0.31	83.55 \pm 0.38	83.45 \pm 0.42	82.37 \pm 0.69	83.59 \pm 0.4	82.29 \pm 0.01	83.72 \pm 0.73
	2%	77.06 \pm 0.35	77.10 \pm 0.12	77.74 \pm 0.51	77.74 \pm 0.43	77.2 \pm 0.56	78.99 \pm 0.73	76.98 \pm 0.66	79.39 \pm 0.49
VGG-19	10%	69.90 \pm 0.26	69.84 \pm 0.15	69.97 \pm 0.43	70.24 \pm 0.29	72.75 \pm 0.22	72.67 \pm 0.01	72.13 \pm 0.08	72.49 \pm 0.33
	5%	68.25 \pm 0.66	68.39 \pm 0.31	68.65 \pm 0.33	68.32 \pm 0.08	71.48 \pm 0.72	71.34 \pm 0.03	71.05 \pm 0.11	71.51 \pm 0.45
	2%	65.98 \pm 0.38	65.68 \pm 0.23	65.87 \pm 0.50	66.00 \pm 0.22	1.00	1.00	48.48 \pm 13.88	53.05 \pm 15.38
ResNet-20	10%	50.66 \pm 0.78	50.97 \pm 0.51	52.29 \pm 0.64	51.80 \pm 0.60	66.90 \pm 0.33	67.11 \pm 0.62	67.32 \pm 0.13	67.52 \pm 0.10
	5%	41.12 \pm 0.92	40.87 \pm 0.76	42.92 \pm 0.53	42.44 \pm 0.48	60.97 \pm 0.45	61.03 \pm 0.03	61.94 \pm 0.60	62.68 \pm 0.32
	2%	23.39 \pm 1.04	23.52 \pm 0.27	24.89 \pm 0.75	24.35 \pm 0.72	47.61 \pm 4.15	48.86 \pm 0.07	50.30 \pm 0.04	51.76 \pm 0.36

unknown parameter w^* established after a learning procedure. Thus, we bound the approximation error with the mask when we apply it to some unknown vector w^* and normally distributed data.

Before we establish our main result, we provide a lemma regarding the error, when the mask is found with some initial vector w^0 and data \tilde{X} but applied on other input data X and weight vector w^* .

Lemma 4.3. *Suppose $X, \tilde{X} \in \mathbb{R}^{d \times n}$, $w^0, w^* \in \mathbb{R}^d$ and $s \in \mathbb{Z}^+$ then when using Algorithm 1 with p^0 and \tilde{X} for m , the error can be bounded as follows*

$$\mathbb{E}_m \left[\|X^T w^* - X^T (w^* \odot m)\|^2 \right] \leq \frac{1}{s} \sum_{k=1}^d \frac{\sum_{j=1}^d \|\tilde{X}_{(j)}\| \|w_j^0\|}{\|\tilde{X}_{(k)}\| \|w_k^0\|} \|X_{(k)}\|^2 w_k^{*2}$$

Next, we show the main result about the error of the mask for unknown parameters and random data.

Theorem 4.4. *Suppose $X \in \mathbb{R}^{d \times n} \sim \frac{1}{\sqrt{n}} \mathcal{N}(0, I)$, $w^0, w^* \in \mathbb{R}^d$ and $s \in \mathbb{Z}^+$ then when using Algorithm 1 with p^0 for m the error can be bounded as follows*

$$\mathbb{E}_X \left[\|X^T w^* - X^T (w^* \odot m)\|^2 \right] \leq \frac{1}{s} \|w^0\|_1 \left(\frac{\|w^* - w^0\|^2}{\|w^0\|_\infty} + 2\|w^* - w^0\|_1 + \|w^0\|_1 \right).$$

To ensure that the bound of Theorem 4.4 is meaningful, we compare it to a simple baseline: The error bound when the mask is sampled uniformly at random.

Lemma 4.5. *Suppose $X \in \mathbb{R}^{d \times n} \sim \frac{1}{\sqrt{n}} \mathcal{N}(0, I)$, $w^0 \in \mathbb{R}^d$ and $s \in \mathbb{Z}^+$. Then when choosing m uniformly at random the error can be bounded as follows*

$$\mathbb{E}_X \left[\|X^T w^* - X^T (w^* \odot m)\|^2 \right] \leq \frac{d}{s} \|w^*\|^2 = \frac{d}{s} \left(\|w^* - w^0\|^2 + 2w^{*T} w^0 \right) - \frac{d}{s} \|w^0\|^2.$$

According to Lemma 4.5, we have an additional dimension factor d that is avoided in Theorem 4.4. Note that Theorem 4.4 bounds the expected error only as a function of the distance between the final vector w^* , w^0 and the properties of the initialization. In Section 7, we use the claim that DNNs under common NTK assumptions do not change much during training. Thus, the error bound is reasonable.

5 SynFlow and Sketching

In this section we analyse theoretically the connection between SynFlow [61] and sketching in the linear case. We calculate the scores given by SynFlow and treat them as probabilities.

SynFlow performs a forward pass on the model with a vector of ones as input and the absolute values of the initialized parameters. The scores are then calculated after summing up all the output features:

$$R_{SF} = \mathbf{1}^T f(\mathbf{1}; |w|), \quad (3)$$

where $\mathbf{1}$ is an all-one vector and the multiplication with it leads to summing all outputs. In order to establish the connection to sketching, we analyse SynFlow scores with $\|X_{(i)}\|$ as input instead of $\mathbf{1}$:

$$R_{SF} = \mathbf{1}^T f(\|X_{(i)}\|; |w|). \quad (4)$$

Note that in the linear model case, where $w \in \mathbb{R}^d$, it holds that

$$R_{SF} = (\|X_{(1)}\|, \|X_{(2)}\|, \dots, \|X_{(i)}\|, \dots, \|X_{(d)}\|) |w|.$$

Hence, it turns out that the SynFlow score for each weight in w is:

$$\frac{\partial R_{SF}}{\partial |w|_i} \odot |w|_i = \|X_{(i)}\| |w|_i,$$

which yields that when looking at the scores as a distribution $p_i \propto \|X_{(i)}\| |w|_i$. Note that in sketching, the probability p_i^0 , as defined in Equation (2), is proportional to the same term and yields the lowest expected approximation error [18]. Thus, it means that in the linear features setting the SynFlow scores and the optimal probability for sketching share the same properties. Hence, if one uses randomization over the mask with SynFlow scores as in Algorithm 1, we get the sketching algorithm. Since we established the equivalence between sketching and SynFlow, all the claims in Section 4 hold for it in the linear case. Note that in Theorem 4.4, we assume random normal data as input. According to Equation (4), SynFlow inputs are $\sqrt{\sum_{i=1}^n \frac{1}{n} x_i^2}$, where x_i are random normal, which implies a χ distribution vector for its input. To summarize, the relation to sketching suggests that we should apply SynFlow with random sampling and χ distribution for its input. We demonstrate the advantage of this approach in Section 8. Sample the entries based on p have the same computation complexity as finding the weights with the largest s scores.

6 SNIP and Sketching

In this section we turn to analyze another well-known method of pruning at initialization named SNIP [39], which aims to estimate the importance of each weight according to its magnitude and gradient magnitude at initialization. The magnitude of the gradient is calculated with respect to input data, \mathcal{D} . SNIP assigns the following saliency score of mask at index j :

$$g_j(w; \mathcal{D}) = \left| \frac{\partial L(m \odot w; \mathcal{D})}{\partial m_j} \right|,$$

where L is the loss used for training and the value of the mask before pruning is 1 in all its entries. We analyse the case of ℓ_1 loss for inputs X . Previously, a statistical justification for using ℓ_1 loss for DNN classification was proven [34] and it was further shown that using ℓ_1 loss can be beneficial for robust classification [26]. The weights' saliency score in the linear model is

$$g_j(w; X, y) = \frac{1}{n} \left| \frac{\partial \sum_{i=1}^n |x_i^T (w \odot m - y_i)|}{\partial m_j} \right| = \frac{1}{n} |w_j| \left| \sum_{i=1}^n \text{sign}(x_i^T w - y_i) x_{ij} \right|.$$

For data which has only one non-zero entry in each row of X , i.e. $\|X_{(j)}\|_0 = 1$, it holds that the induced probability is $p_j = \frac{|w_j| |x_{ij, \text{s.t. } x_{ij} \neq 0}|}{\sum_{k=1}^d |w_k| |x_{ik, \text{s.t. } x_{ik} \neq 0}|} = \frac{|w_j| \|X_{(j)}\|}{\sum_{k=1}^d |w_k| \|X_{(k)}\|}$. The induced probability in this case is optimal from a sketching perspective. Thus, in the unsupervised case, we should apply SNIP with random sparse data and random sampling of the mask. We validate this conclusion empirically in Section 8.

7 Neural Tangent Kernel Pruning

We turn to apply our sketching results to the NTK regime [37, 32, 6], which was introduced for examining the training dynamics of DNNs. Under infinite width assumption, the gradient descent steps over a DNN become analytically tractable and similar to learning with a known kernel.

Table 2: Accuracy results with GraSP [63] and Iterative Magnitude Pruning (IMP) [23] with random data used for pruning and mask randomization that replaces the thresholding. Reported accuracy results with CIFAR-10 (top) and CIFAR-100 (bottom). We provide the supervised version of the methods as reference and we boldface the best method with random data.

Model Density	VGG-19			ResNet-20		
	10%	5%	2%	10%	5%	2%
Random	91.14 ± 0.08	89.24 ± 0.22	86.28 ± 0.04	85.04 ± 0.12	72.08 ± 1.38	10.0
Magnitude	93.05 ± 0.22	92.23 ± 0.9	91.28 ± 0.43	84.88 ± 0.7	81.97 ± 0.52	75.15 ± 0.86
GraSP (supervised)	92.21 ± 0.69	91.68 ± 1.21	90.92 ± 1.28	87.28 ± 0.04	84.37 ± 0.21	79.53 ± 0.06
GraSP + normal data	92.23 ± 0.95	91.23 ± 0.91	90.9 ± 1.63	86.3 ± 0.46	83.61 ± 0.13	79.59 ± 0.1
GraSP + normal data + rand. mask	92.12 ± 0.88	91.57 ± 1.1	91.22 ± 1.08	86.59 ± 0.29	84.35 ± 1.34	78.36 ± 0.16
IMP (supervised)	93.56 ± 0.19	92.64 ± 0.19	89.63 ± 1.57	89.63 ± 0.24	85.99 ± 1.3	82.46 ± 0.73
IMP + rand. data	91.53 ± 0.32	91.42 ± 0.19	90.58 ± 0.69	85.46 ± 0.11	83.07 ± 0.11	77.97 ± 0.04
IMP + rand. data + rand mask	91.57 ± 0.03	91.45 ± 0.12	90.55 ± 0.7	85.5 ± 0.15	82.77 ± 0.13	77.54 ± 0.49
Random	66.02 ± 0.13	62.7 ± 0.57	58.28 ± 0.25	51.09 ± 0.43	26.61 ± 3.51	1.0 ± 0.0
Magnitude	69.43 ± 0.49	68.09 ± 0.21	65.18 ± 0.47	52.03 ± 0.24	45.64 ± 0.4	32.9 ± 0.65
GraSP (supervised)	70.64 ± 0.43	70.03 ± 0.55	67.78 ± 0.42	67.24 ± 0.23	63.08 ± 0.33	53.18 ± 0.94
GraSP + normal data	70.52 ± 0.18	70.06 ± 0.29	68.07 ± 0.16	67.37 ± 0.02	63.66 ± 0.06	54.15 ± 0.63
GraSP + normal data + rand. mask	71.15 ± 0.32	70.08 ± 0.01	68.53 ± 0.18	67.39 ± 0.46	64.34 ± 0.15	53.79 ± 0.16
IMP (supervised)	70.88 ± 0.96	69.87 ± 1.28	67.9 ± 1.36	58.38 ± 2.97	50.39 ± 0.16	40.88 ± 0.22
IMP + rand. data	66.84 ± 0.16	66.23 ± 0.17	54.81 ± 6.87	51.66 ± 0.68	43.84 ± 0.17	32.92 ± 0.65
IMP + rand. data + rand. mask	67.1 ± 0.21	65.3 ± 0.23	59.05 ± 0.14	52.05 ± 0.6	44.68 ± 0.38	33.37 ± 0.74

The NTK assumptions allows representing the DNN features in a linearized manner. Hence, we can apply our previous results with sketching. Before doing that we provide some basic NTK definitions.

NTK definitions. We use the same notations as appeared in [37]: $\theta_t \in \mathbb{R}^d$ is the vectorization of the parameters at time t ; $f_t(x) \in \mathbb{R}^m$ is the output of the model at time t ; $(\mathcal{X}, \mathcal{Y})$ are the input vectors and labels (we assume that $\mathcal{Y}_i \in \mathbb{R}$); $f_t(\mathcal{X})$ is a concatenation of all outputs; n is the notion of width of the model; $J(\theta_t) = \nabla_{\theta} f_t(\mathcal{X}) \in \mathbb{R}^{|\mathcal{X}|m \times d}$ is the Jacobian; $\hat{\Theta}_t = \nabla_{\theta} f_t(\mathcal{X}) \nabla_{\theta} f_t(\mathcal{X})^T = \frac{1}{n} J(\theta_t) J(\theta_t)^T$ is the empirical NTK. We refer to the analytic kernel as $\Theta = \lim_{n \rightarrow \infty} \hat{\Theta}_0$.

For the claims in [37] to hold we use assumptions that are based on the original paper: **(i)** The empirical NTK converges in probability to the analytic NTK: $\hat{\Theta}_0 \rightarrow_{n \rightarrow \infty} \Theta$; **(ii)** The analytic NTK Θ is full rank. $0 < \lambda_{\min} \leq \lambda_{\max} < \infty$ and let $\eta_{critical} = 2(\lambda_{\min} + \lambda_{\max})^{-1}$; **(iii)** $(\mathcal{X}, \mathcal{Y})$ is a compact set and for $x, \tilde{x} \in \mathcal{X}$, $x \neq \tilde{x}$; and **(iv)** The Jacobian is locally Lipschitz as defined in Definition 7.1 (originally stated in [37, Lemma 2]):

Definition 7.1 (Local Lipschitzness of the Jacobian). *Denote $B(\theta_0, C) = \{\theta : \|\theta - \theta_0\| \leq C\}$. The Jacobian is locally Lipschitz if there exists $K > 0$ such that for every $C > 0$, with high probability over random initialization the following holds for $\theta, \tilde{\theta} \in B(\theta_0, C)$*

$$\|J(\theta) - J(\tilde{\theta})\|_F \leq K \|\theta - \tilde{\theta}\| \quad \text{and} \quad \|J(\theta)\|_F \leq K.$$

Note that local Lipschitzness constants are usually determined by the DNN activation functions.

NTK Pruning. We focus on the linearized approximation $f_t^{lin}(x) = \nabla_{\theta_t} f_t(x) \theta_t$ of the model features. We aim to find a mask to apply on θ_t according to the linear features of the network at initialization, $f_0^{lin}(\mathcal{X})$ and θ_0 , using sketching as in Algorithm 1. Thus, we can use our previous analysis to bound the error induced by the mask on the features at time t , $f_t^{lin}(x)$. The following theorem relies on the NTK bounds in [37, Theorem G.4]. Our theorem proof is in Appendix B.6.

Theorem 7.2. *Under assumptions [i-iv], $\delta_0 > 0$ and $\eta_0 \leq \eta_{critical}$, let $F(A) = \sum_{i=1}^d \frac{1}{\|A^{(i)}\|}$ and $m \in \mathbb{R}^d$ be a s -dense mask found with Algorithm 1 with p according to $f_0^{lin}(\mathcal{X})$ and θ_0 (Equation (2)). Then there exist $R_0 > 0$, $K > 1$ such that for every $n \geq N$ the following holds with probability $> 1 - \delta_0$ over random initialization when applying GD with learning rate of η_0 :*

$$\begin{aligned} & \mathbb{E}_m \left[\left\| f_t^{lin}(\mathcal{X}) - \nabla_{\theta_t} f_t(\mathcal{X}) (\theta_t \odot m) \right\|^2 \right] \\ & \leq \frac{1}{s} K^3 \|\theta_0\|_1 F(J(\theta_0)) \left(\|\theta_0\|_1 + F(\theta_0) \frac{9K^4 R_0^2}{\lambda_{\min}^2} + 6\sqrt{d} \frac{K^3 R_0}{\lambda_{\min}} \right). \end{aligned}$$

Note that for a mask density of $s = O(\sqrt{d})$, the error of using the mask at time t only depends on the initialization and constants from the NTK assumptions. Additionally, $\nabla_{\theta_t} f_t(\mathcal{X}) (\theta_t \odot m)$ are the

masked linearized outputs of the model at time t . We prove the above theorem using the bound on the Jacobian norm and the claim that under the conditions of [37, Theorem G.4] it is guaranteed that the distance of the parameters at time t , θ_t , from the parameters at initialization, θ_0 , is bounded.

8 Experiments

We study our theoretical insights empirically on sparse DNNs. We tested multiple pruning at initialization methods: SynFlow [61], SNIP [39], GraSP [63] and Iterative Magnitude Pruning (IMP), the algorithm suggested for finding the winning lottery ticket [23].

We use CIFAR-10/100 [35] and Tiny-ImageNet [66] with VGG-19 [59], ResNet-20 [30] and WideResNet-20-32 [69]. We employ SGD with momentum, batch size 128, and learning rate 0.1 multiplied by 0.1 after epoch 80 and 120. We train the models for 160 epochs with weight decay 10^{-4} . For Tiny-ImageNet, we use a modified version of ResNet-18 and WideResNet-18. Our code is based on the repositories of [22, 61, 60]. All the experiments performed on a single NVIDIA GeForce RTX 2080 Ti.

We found the SynFlow mask using 100 iterations. We employ SNIP and GraSP with batch size of 256. For IMP, we use 1000 iterations of warmup for VGG-19 and 2000 iterations for ResNet-20 with CIFAR-10 and 6000 for CIFAR-100 with ResNet20. In the unsupervised experiments, we examples are drawn from a normal distribution with the same expectation and standard deviation of the original dataset. All the results include the average and standard deviation of 3 different seeds.

The mask randomization is performed in three steps. The first is to compute the threshold according to the number of desired remaining weights. The second is to compute the number of remaining weights within each layer with respect to hard thresholding. Finally, the third step is to randomly select a mask for each layer according to the granularity found in the previous step and the scores of the pruning method. We randomize the mask in this manner due to computational limitations.

Figure 1a shows that the magnitudes of the weights chosen by SynFlow and IMP are larger than a uniform random choice of parameters. Note that SynFlow has a stronger bias towards larger magnitudes than IMP. Figure 2 presents a case, where the IMP mask has an extremely high norms compared to random masks and the high norm is maintained across sparsities. We test the effect of randomizing the mask on the chosen scores. Figure 1b presents a comparison of the histogram of scores of weights chosen with SynFlow with and without randomization compared to the distribution of all the scores in the network. We report the scores of VGG-19 with CIFAR-10 and for simplicity we present the results only on a subset of 1000 weights chosen uniformly at random.

To show the effect of changes used in the theoretical analysis we tested SynFlow with mask randomization and replacing the all-one vector with χ distributed random data. We generate the χ distribution according to the ℓ_2 norms of a vector with normally distributed variables and dimension $n = 128$. We randomize data at each pruning iteration. In order to validate empirically the conclusion in Section 6 for the relation between SNIP and sketching, we tested SNIP with sparse random data. We choose randomly for each input pixel location, a single image in the batch where the pixel is non-zero. Note that the images are drawn from a normal distribution and are not natural images. Table 1 shows that replacing the thresholding with a random mask and replacing the input with the distribution derived from our analysis improve results in most cases when compared to the original SynFlow and naive data-independent SNIP. For SynFlow, the use of mask randomization leads to improved performance. The combination of sparse data and mask randomization leads to superior accuracy for SNIP. It suggests that our sampling of mask and data can be used and improve other pruning methods based on it, e.g. [2, 17]. Additional results with the original supervised SNIP found in the Appendix A. Most accuracy results with random masks and sparse data outperform SNIP even with labeled input.

Table 3: Result with SynFlow and mask randomization for Tiny-ImageNet.

Model	Density	SynFlow	SynFlow + random mask
ResNet-18	10%	58.3	60.64
	5%	57.63	58.57
	2%	54.62	55.56
WideResNet	10%	59.25	60.22
	5%	57.49	58.84
	2%	54.8	55.54

Our claim that finding a good sparse subnetwork at initialization does not necessarily depend on the data is tested by an experiment where the masks are learned with completely random input and then retrained with real supervised data. Table 2 reports the accuracy results with CIFAR-10/100. We can see that randomized masks produce comparable and usually better results than pruning methods with random data. Also, it can be seen that, indeed, the performance of data dependent pruning methods is only partially explained by the use of supervised input data, as shown in [60]. Note that it is expected to see some degradation in accuracy since those methods are designed to work with labeled data.

For training with Tiny-ImageNet the improvement in performance is clear with the mask randomization inspired by sketching, see Table 3. The improvement in accuracy is around 1% for all sparsities and architectures tested. Overall, randomizing the masks leads to a new the state-of-the-art with SynFlow.

9 Conclusion and Future Work

This work presents and analyzes the task of pruning at initialization from the perspective of sketching. Based on our theoretical study, we gain a new justification for the claim that good sparse subnetworks are data independent. Additionally, we apply ideas from sketching to DNNs. Our proposed changes can be added to existing and future pruning methods.

While we have proposed a novel connection between pruning at initialization and sketching, our framework has some limitations. We apply our approach, only in the setting of pruning at initialization. One might investigate our suggested approach to other settings of pruning after or during training and structured pruning methods. In addition, we have studied only one sketching approach. We leave for future work exploiting more complex sketching methods, which possibly can lead to new insights and improvements to DNN pruning. Also, future research may be conducted to generalize the rather simple linear features framework to a deeper model where the search space for the mask is even larger. The search space in this case might be ambiguous, i.e., two different masks can lead to the same output [72]. We believe that the relationship we draw here can be used in many other directions besides those indicated above and contribute to DNN understanding and pruning.

Acknowledgements

This work is supported by the European research council under Grant ERC-StG 757497 and by Tel Aviv University Center for AI and Data Science (TAD).

References

- [1] Mohamed S Abdelfattah, Abhinav Mehrotra, Łukasz Dudziak, and Nicholas D Lane. Zero-cost proxies for lightweight nas. *arXiv preprint arXiv:2101.08134*, 2021.
- [2] Milad Alizadeh, Shyam A Tailor, Luisa M Zintgraf, Joost van Amersfoort, Sebastian Farquhar, Nicholas Donald Lane, and Yarin Gal. Prospect pruning: Finding trainable weights at initialization using meta-gradients. *arXiv preprint arXiv:2202.08132*, 2022.
- [3] Sanjeev Arora, Nadav Cohen, Noah Golowich, and Wei Hu. A convergence analysis of gradient descent for deep linear neural networks. In *International Conference on Learning Representations*, 2019.
- [4] Sanjeev Arora, Nadav Cohen, and Elad Hazan. On the optimization of deep networks: Implicit acceleration by overparameterization. In *International Conference on Machine Learning*, pages 244–253. PMLR, 2018.
- [5] Sanjeev Arora, Nadav Cohen, Wei Hu, and Yuping Luo. Implicit regularization in deep matrix factorization. In *Advances in Neural Information Processing Systems (NeurIPS)*, pages 7413–7424, 2019.

- [6] Sanjeev Arora, Simon Du, Wei Hu, Zhiyuan Li, and Ruosong Wang. Fine-grained analysis of optimization and generalization for overparameterized two-layer neural networks. In *International Conference on Machine Learning*, pages 322–332. PMLR, 2019.
- [7] Sanjeev Arora, Rong Ge, Behnam Neyshabur, and Yi Zhang. Stronger generalization bounds for deep nets via a compression approach. In *International Conference on Machine Learning*, pages 254–263. PMLR, 2018.
- [8] Guillaume Bellec, David Kappel, Wolfgang Maass, and Robert Legenstein. Deep rewiring: Training very sparse deep networks. In *International Conference on Learning Representations*, 2018.
- [9] Alon Brutzkus, Amir Globerson, Eran Malach, and Shai Shalev-Shwartz. SGD learns overparameterized networks that provably generalize on linearly separable data. In *International Conference on Learning Representations*, 2018.
- [10] Rebekka Burkholz, Nilanjana Laha, Rajarshi Mukherjee, and Alkis Gotovos. On the existence of universal lottery tickets. In *International Conference on Learning Representations*, 2021.
- [11] Miguel A Carreira-Perpinán and Yerlan Idelbayev. “learning-compression” algorithms for neural net pruning. In *Proceedings of the IEEE Conference on Computer Vision and Pattern Recognition*, pages 8532–8541, 2018.
- [12] Yves Chauvin. A back-propagation algorithm with optimal use of hidden units. *Advances in neural information processing systems*, 1, 1988.
- [13] Tianlong Chen, Jonathan Frankle, Shiyu Chang, Sijia Liu, Yang Zhang, Michael Carbin, and Zhangyang Wang. The lottery tickets hypothesis for supervised and self-supervised pre-training in computer vision models. In *CVPR*, 2021.
- [14] Tianyi Chen, Bo Ji, Tianyu Ding, Biyi Fang, Guanyi Wang, Zhihui Zhu, Luming Liang, Yixin Shi, Sheng Yi, and Xiao Tu. Only train once: A one-shot neural network training and pruning framework. *Advances in Neural Information Processing Systems*, 34:19637–19651, 2021.
- [15] Tianyi Chen, Luming Liang, Tianyu DING, Zhihui Zhu, and Ilya Zharkov. OTOv2: Automatic, generic, user-friendly. In *The Eleventh International Conference on Learning Representations*, 2023.
- [16] Daiki Chijiwa, Shin’ya Yamaguchi, Yasutoshi Ida, Kenji Umakoshi, and Tomohiro Inoue. Pruning randomly initialized neural networks with iterative randomization. *arXiv:2106.09269*, 2021.
- [17] Pau de Jorge, Amartya Sanyal, Harkirat S Behl, Philip HS Torr, Gregory Rogez, and Puneet K Dokania. Progressive skeletonization: Trimming more fat from a network at initialization. *arXiv preprint arXiv:2006.09081*, 2020.
- [18] Petros Drineas, Ravi Kannan, and Michael W Mahoney. Fast monte carlo algorithms for matrices i: Approximating matrix multiplication. *SIAM Journal on Computing*, 36(1):132–157, 2006.
- [19] Utku Evci, Trevor Gale, Jacob Menick, Pablo Samuel Castro, and Erich Elsen. Rigging the lottery: Making all tickets winners. In *ICML*. PMLR, 2020.
- [20] Jonas Fischer and Rebekka Burkholz. Towards strong pruning for lottery tickets with non-zero biases. *arXiv preprint arXiv:2110.11150*, 2021.
- [21] Jonas Fischer and Rebekka Burkholz. Plant’n’sseek: Can you find the winning ticket? In *International Conference on Learning Representations*, 2022.
- [22] Jonathan Frankle. Openlth: A framework for lottery tickets and beyond, 2020.
- [23] Jonathan Frankle and Michael Carbin. The lottery ticket hypothesis: Finding sparse, trainable neural networks. In *7th International Conference on Learning Representations, ICLR 2019, New Orleans, LA, USA, May 6-9, 2019*. OpenReview.net, 2019.
- [24] Jonathan Frankle, Gintare Karolina Dziugaite, Daniel Roy, and Michael Carbin. Linear mode connectivity and the lottery ticket hypothesis. In *ICML*, pages 3259–3269. PMLR, 2020.

- [25] Thomas Gebhart, Udit Saxena, and Paul Schrater. A unified paths perspective for pruning at initialization. *arXiv preprint arXiv:2101.10552*, 2021.
- [26] Aritra Ghosh, Himanshu Kumar, and P Shanti Sastry. Robust loss functions under label noise for deep neural networks. In *Proceedings of the AAAI conference on artificial intelligence*, 2017.
- [27] Yiwen Guo, Anbang Yao, and Yurong Chen. Dynamic network surgery for efficient dnns. *Advances in neural information processing systems*, 29, 2016.
- [28] Song Han, Jeff Pool, John Tran, and William Dally. Learning both weights and connections for efficient neural network. *Advances in neural information processing systems*, 28, 2015.
- [29] Babak Hassibi, David G Stork, and Gregory J Wolff. Optimal brain surgeon and general network pruning. In *IEEE international conference on neural networks*, pages 293–299. IEEE, 1993.
- [30] Kaiming He, Xiangyu Zhang, Shaoqing Ren, and Jian Sun. Deep residual learning for image recognition. In *Proceedings of the IEEE conference on computer vision and pattern recognition*, pages 770–778, 2016.
- [31] Nathan Hubens, Matei Mancas, Bernard Gosselin, Marius Preda, and Titus Zaharia. One-cycle pruning: Pruning convnets under a tight training budget. *arXiv:2107.02086*, 2021.
- [32] Arthur Jacot, Franck Gabriel, and Clément Hongler. Neural tangent kernel: Convergence and generalization in neural networks. *Advances in neural information processing systems*, 31, 2018.
- [33] Max Jaderberg, Andrea Vedaldi, and Andrew Zisserman. Speeding up convolutional neural networks with low rank expansions. In *Proceedings of the British Machine Vision Conference*. BMVA Press, 2014.
- [34] Katarzyna Janocha and Wojciech Marian Czarnecki. On loss functions for deep neural networks in classification. *arXiv preprint arXiv:1702.05659*, 2017.
- [35] Alex Krizhevsky. Learning multiple layers of features from tiny images. 2009.
- [36] Yann LeCun, John Denker, and Sara Solla. Optimal brain damage. *Advances in neural information processing systems*, 2, 1989.
- [37] Jaehoon Lee, Lechao Xiao, Samuel Schoenholz, Yasaman Bahri, Roman Novak, Jascha Sohl-Dickstein, and Jeffrey Pennington. Wide neural networks of any depth evolve as linear models under gradient descent. *Advances in neural information processing systems*, 32, 2019.
- [38] Namhoon Lee, Thalaiyasingam Ajanthan, Stephen Gould, and Philip H. S. Torr. A signal propagation perspective for pruning neural networks at initialization. In *ICLR*, 2020.
- [39] Namhoon Lee, Thalaiyasingam Ajanthan, and Philip HS Torr. Snip: Single-shot network pruning based on connection sensitivity. *arXiv preprint arXiv:1810.02340*, 2018.
- [40] Zhiyuan Li, Yuping Luo, and Kaifeng Lyu. Towards resolving the implicit bias of gradient descent for matrix factorization: Greedy low-rank learning. In *International Conference on Learning Representations*, 2021.
- [41] Tianlin Liu and Friedemann Zenke. Finding trainable sparse networks through neural tangent transfer. In *International Conference on Machine Learning*, pages 6336–6347. PMLR, 2020.
- [42] Christos Louizos, Max Welling, and Diederik P. Kingma. Learning sparse neural networks through l_0 regularization. In *International Conference on Learning Representations*, 2018.
- [43] Eran Malach, Gilad Yehudai, Shai Shalev-Schwartz, and Ohad Shamir. Proving the lottery ticket hypothesis: Pruning is all you need. In *ICML*. PMLR, 2020.
- [44] Joe Mellor, Jack Turner, Amos Storkey, and Elliot J Crowley. Neural architecture search without training. In *International Conference on Machine Learning*, pages 7588–7598. PMLR, 2021.
- [45] Decebal Constantin Mocanu, Elena Mocanu, Peter Stone, Phuong H Nguyen, Madeleine Gibescu, and Antonio Liotta. Scalable training of artificial neural networks with adaptive sparse connectivity inspired by network science. *Nature communications*, 9(1):2383, 2018.

- [46] Pavlo Molchanov, Stephen Tyree, Tero Karras, Timo Aila, and Jan Kautz. Pruning convolutional neural networks for resource efficient inference. *arXiv preprint arXiv:1611.06440*, 2016.
- [47] Ari Morcos, Haonan Yu, Michela Paganini, and Yuandong Tian. One ticket to win them all: generalizing lottery ticket initializations across datasets and optimizers. In *NeurIPS*, 2019.
- [48] Hesham Mostafa and Xin Wang. Parameter efficient training of deep convolutional neural networks by dynamic sparse reparameterization. In *International Conference on Machine Learning*, pages 4646–4655. PMLR, 2019.
- [49] Michael C Mozer and Paul Smolensky. Skeletonization: A technique for trimming the fat from a network via relevance assessment. *Advances in neural information processing systems*, 1, 1988.
- [50] Mor Shpigel Nacson, Kavya Ravichandran, Nathan Srebro, and Daniel Soudry. Implicit bias of the step size in linear diagonal neural networks. In *International Conference on Machine Learning*, volume 162, pages 16270–16295, 17–23 Jul 2022.
- [51] James O’ Neill. An overview of neural network compression. *arXiv preprint arXiv:2006.03669*, 2020.
- [52] Alexander Novikov, Dmitrii Podoprikin, Anton Osokin, and Dmitry P Vetrov. Tensorizing neural networks. *Advances in neural information processing systems*, 28, 2015.
- [53] Laurent Orseau, Marcus Hutter, and Omar Rivasplata. Logarithmic pruning is all you need. *Advances in Neural Information Processing Systems*, 33:2925–2934, 2020.
- [54] Shreyas Malakarjun Patil and Constantine Dovrolis. Phew: Constructing sparse networks that learn fast and generalize well without training data. In *International Conference on Machine Learning*, pages 8432–8442. PMLR, 2021.
- [55] Ankit Pensia, Shashank Rajput, Alliot Nagle, Harit Vishwakarma, and Dimitris Papailiopoulos. Optimal lottery tickets via subsetsum: Logarithmic over-parameterization is sufficient. *arXiv:2006.07990*, 2020.
- [56] Vivek Ramanujan, Mitchell Wortsman, Aniruddha Kembhavi, Ali Farhadi, and Mohammad Rastegari. What’s hidden in a randomly weighted neural network? In *CVPR*, pages 11893–11902, 2020.
- [57] Matthia Sabatelli, Mike Kestemont, and Pierre Geurts. On the transferability of winning tickets in non-natural image datasets. *arXiv:2005.05232*, 2020.
- [58] Ohad Shamir. Exponential convergence time of gradient descent for one-dimensional deep linear neural networks. In *Conference on Learning Theory*, volume 99, pages 2691–2713, 25–28 Jun 2019.
- [59] Karen Simonyan and Andrew Zisserman. Very deep convolutional networks for large-scale image recognition. *arXiv preprint arXiv:1409.1556*, 2014.
- [60] Jingtong Su, Yihang Chen, Tianle Cai, Tianhao Wu, Ruiqi Gao, Liwei Wang, and Jason D Lee. Sanity-checking pruning methods: Random tickets can win the jackpot. *arXiv:2009.11094*, 2020.
- [61] Hidenori Tanaka, Daniel Kunin, Daniel L Yamins, and Surya Ganguli. Pruning neural networks without any data by iteratively conserving synaptic flow. *Advances in Neural Information Processing Systems*, 33:6377–6389, 2020.
- [62] Joost van Amersfoort, Milad Alizadeh, Sebastian Farquhar, Nicholas Lane, and Yarín Gal. Single shot structured pruning before training. *arXiv preprint arXiv:2007.00389*, 2020.
- [63] Chaoqi Wang, Guodong Zhang, and Roger Grosse. Picking winning tickets before training by preserving gradient flow. *arXiv preprint arXiv:2002.07376*, 2020.
- [64] Colin White, Arber Zela, Robin Ru, Yang Liu, and Frank Hutter. How powerful are performance predictors in neural architecture search? *Advances in Neural Information Processing Systems*, 34:28454–28469, 2021.

- [65] Cameron R Wolfe, Qihan Wang, Junhyung Lyle Kim, and Anastasios Kyrillidis. Provably efficient lottery ticket discovery. *arXiv:2108.00259*, 2021.
- [66] Jiayu Wu, Qixiang Zhang, and Guoxi Xu. Tiny imagenet challenge. *Technical report*, 2017.
- [67] Haoran You, Chaojian Li, Pengfei Xu, Yonggan Fu, Yue Wang, Xiaohan Chen, Richard G Baraniuk, Zhangyang Wang, and Yingyan Lin. Drawing early-bird tickets: Towards more efficient training of deep networks. *arXiv:1909.11957*, 2019.
- [68] Chulhee Yun, Shankar Krishnan, and Hossein Mobahi. A unifying view on implicit bias in training linear neural networks. In *International Conference on Learning Representations*, 2021.
- [69] Sergey Zagoruyko and Nikos Komodakis. Wide residual networks. *arXiv preprint arXiv:1605.07146*, 2016.
- [70] Zeru Zhang, Jiayin Jin, Zijie Zhang, Yang Zhou, Xin Zhao, Jiaxiang Ren, Ji Liu, Lingfei Wu, Ruoming Jin, and Dejing Dou. Validating the lottery ticket hypothesis with inertial manifold theory. *Advances in Neural Information Processing Systems*, 34:30196–30210, 2021.
- [71] Zhenyu Zhang, Xuxi Chen, Tianlong Chen, and Zhangyang Wang. Efficient lottery ticket finding: Less data is more. In *ICML*, pages 12380–12390. PMLR, 2021.
- [72] Léon Zheng, Elisa Riccietti, and Rémi Gribonval. Identifiability in two-layer sparse matrix factorization. *complexity*, 20(19):28–29, 2021.

A Results with Supervised SNIP

Table 4: Accuracy results with the original supervised SNIP and unsupervised SNIP with sparse data and mask randomization. Above are results with CIFAR-10 and below are results with CIFAR-100.

Model Density	10%	VGG-19 5%	2%	10%	ResNet20 5%	2%
SNIP (supervised)	92.62 ± 0.09	91.66 ± 0.25	90.92 ± 0.16	86.29 ± 0.92	82.55 ± 1.02	78.16 ± 0.8
SNIP + sparse data + rand. mask	93.16 ± 0.36	92.79 ± 0.78	92.03 ± 0.91	87.02 ± 0.65	83.72 ± 0.73	79.39 ± 0.49
SNIP (supervised)	71.80 ± 0.66	71.07 ± 0.23	56.05 ± 13.97	67.03 ± 0.04	61.80 ± 0.38	49.42 ± 0.65
SNIP + sparse data + rand. mask	72.49 ± 0.33	71.51 ± 0.45	53.05 ± 15.38	67.52 ± 0.10	62.68 ± 0.32	51.76 ± 0.36

B Proofs for Sketching and SynFlow

In this section we include the proofs of the claims presented in the main paper regarding the SynFlow and sketching.

B.1 Useful Lemmas and Proofs

First we present useful lemmas and proofs that are used to prove the lemmas and theorems in the paper.

We calculate the expectation of the mask with some unknown w^* vector.

Lemma B.1. For m found with Algorithm 1 and p^0 . Then for $w^* \in \mathbb{R}^d$ it holds,

$$\mathbb{E}[(X^T(w^* \odot m))_i] = (X^T w^*)_i$$

Lemma B.1. Fix an index i and denote the random variable $Y_t^{0*} = \frac{X_{i_t} w_{i_t}^*}{s p_{i_t}^0}$ (i_t is random and hence $p_{i_t}^0$ is random), it holds that $\sum_{t=1}^s Y_t^{0*} = \sum_{t=1}^d X_{i_t} w_{i_t}^* \cdot \frac{1}{s p_{i_t}^0} = (X^T(w^* \odot m))_i$.

$$\mathbb{E}_{i_t}[Y_t^{0*}] = \sum_{k=1}^d p_k^0 \frac{X_{ki} w_k^*}{s p_k^0} = \frac{1}{s} (X_{(i)}^T w^*) = \frac{1}{s} (X^T w^*)_i.$$

Sum over s random variables we have

$$\mathbb{E}_{i_t}[(X^T(w^* \odot m))_i] = \sum_{t=1}^s \mathbb{E}[Y_t^{0*}] = (X^T w^*)_i.$$

□

We calculate the variance of each mask entry when the mask is applied on w^* .

Lemma B.2. For m found with Algorithm 1 with p^0 . Then for $w_* \in \mathbb{R}^d$ it holds,

$$\text{Var}[(X^T(w^* \odot m))_i] = \frac{1}{s} \sum_{k=1}^d \frac{(X_{ki})^2 (w_k^*)^2}{p_k^0} - \frac{1}{s} (X^T w^*)_i^2$$

Lemma B.2. According to the variance of independent variables

$$\text{Var}[(X^T(w^* \odot m))_i] = \sum_{t=1}^s \text{Var}[Y_t^{0*}] = \sum_{t=1}^s \mathbb{E}[(Y_t^{0*})^2] - \mathbb{E}[Y_t^{0*}]^2.$$

Then we focus on $\mathbb{E}[(Y_t^{0*})^2]$ calculation,

$$\mathbb{E}[(Y_t^{0*})^2] = \sum_{k=1}^d \frac{(X_{ki})^2 (w_k^*)^2}{s^2 p_k^0}.$$

Then the use of Lemma B.2 concludes the proof.

□

B.2 Proof of Lemma 4.3

The following lemma supports Theorem 4.4 and Theorem 7.2. This lemma establish the variance of each masked entry when the mask is found with w^0 and \tilde{X} but applied on other input data and weight vector.

Lemma 4.3. *Suppose $X, \tilde{X} \in \mathbb{R}^{d \times n}$, $w^0, w^* \in \mathbb{R}^d$ and $s \in \mathbb{Z}^+$ then when using Algorithm 1 with p^0 and \tilde{X} for m the error can be bounded*

$$\begin{aligned} \mathbb{E}_m \left[\|X^T w^* - X^T(w^* \odot m)\|^2 \right] &= \frac{1}{s} \sum_{k=1}^d \frac{1}{p_k^0} \|X_{(k)}\|^2 w_k^{*2} - \frac{1}{s} \|X^T w^*\|^2 \\ &\leq \frac{1}{s} \sum_{k=1}^d \frac{\sum_{j=1}^d \|\tilde{X}_{(j)}\| |w_j^0|}{\|\tilde{X}_{(k)}\| |w_k^0|} \|X_{(k)}\|^2 w_k^{*2} \end{aligned}$$

Proof. m is drawn i.i.d.

$$\begin{aligned} \mathbb{E}_m \left[\|X^T w^* - X^T(w^* \odot m)\|^2 \right] &= \sum_{i=1}^n \mathbb{E}_m \left[(X^T w^* - X^T(w^* \odot m))_i^2 \right] \\ &= \sum_{i=1}^n (X^T w^*)_i^2 - 2(X^T w^*)_i \mathbb{E}_m \left[(X^T(w^* \odot m))_i \right] + \mathbb{E}_m \left[(X^T(w^* \odot m))_i^2 \right] \\ &\stackrel{\text{Lemma B.1}}{=} \sum_{i=1}^n \text{Var}_m \left[(X^T(w^* \odot m))_i \right] \\ &\stackrel{\text{Lemma B.2}}{=} \frac{1}{s} \sum_{k=1}^d \frac{1}{p_k^0} \left(\sum_{i=1}^n X_{ki}^2 \right) (w_k^*)^2 - \frac{1}{s} \|X^T w^*\|^2 \\ &\leq \frac{1}{s} \sum_{k=1}^d \frac{1}{p_k^0} \left(\sum_{i=1}^n X_{ki}^2 \right) (w_k^*)^2 \\ &\stackrel{p^0 \text{ definition}}{=} \frac{1}{s} \sum_{k=1}^d \frac{\sum_{j=1}^d \|\tilde{X}_{(j)}\| |w_j^0|}{\|\tilde{X}_{(k)}\| |w_k^0|} \|X_{(k)}\|^2 w_k^{*2} \end{aligned}$$

□

Now, we can repeat the lemmas and theorem from the main paper and present their proofs.

B.3 Proof of Lemma 4.2

Lemma 4.2. *Suppose $X \in \mathbb{R}^{d \times n} \sim \frac{1}{\sqrt{n}} \mathcal{N}(0, I)$, $w^0 \in \mathbb{R}^d$ and $s \in \mathbb{Z}^+$ then when using Algorithm 1 with p^0 for m the error can be bounded*

$$\mathbb{E}_X \left[\|X^T w^0 - X^T(w^0 \odot m)\|^2 \right] \leq \frac{1}{s} \|w^0\|^2$$

Proof.

$$\begin{aligned}
\mathbb{E}_X \left[\|X^T w^0 - X^T (w^0 \odot m)\|^2 \right] &= \mathbb{E}_X \left[\mathbb{E}_{m|X} \left[\|X^T w^0 - X^T (w^0 \odot m)\|^2 \right] \right] \\
&\stackrel{\text{Lemma 4.1}}{=} \mathbb{E}_X \left[\frac{1}{s} \left(\sum_{k=1}^d \|X_{(k)}\| |w_k^0| \right)^2 - \frac{1}{s} \|X^T w^0\|^2 \right] \\
&\leq \mathbb{E}_X \left[\frac{1}{s} \left(\sum_{k=1}^d \|X_{(k)}\| |w_k^0| \right)^2 \right] \\
&\leq \frac{1}{s} \mathbb{E}_X \left[\sum_{k=1}^d \|X_{(k)}\|^2 (w_k^0)^2 \right] \\
&= \frac{1}{s} \sum_{k=1}^d \mathbb{E}_X \left[\|X_{(k)}\|^2 \right] (w_k^0)^2 = \frac{n}{sn} \|w^0\|^2
\end{aligned}$$

□

B.4 Proof of Theorem 4.4

Theorem 4.4. *Suppose $X \in \mathbb{R}^{d \times n} \sim \frac{1}{\sqrt{n}} \mathcal{N}(0, I)$, $w^0, w^* \in \mathbb{R}^d$ and $s \in \mathbb{Z}^+$ then when using Algorithm 1 with p^0 for m the error can be bounded*

$$\begin{aligned}
&\mathbb{E}_X \left[\|X^T w^* - X^T (w^* \odot m)\|^2 \right] \\
&\leq \frac{1}{s} \|w^0\|_1 \left(\frac{\|w^* - w^0\|^2}{\|w^0\|_\infty} + 2\|w^* - w^0\|_1 + \|w^0\|_1 \right).
\end{aligned}$$

Proof. We calculate the expectation over X . Since X rows are i.i.d. we replace $\mathbb{E}\|X_{(k)}\|$ in $\mathbb{E}\|X_{(\cdot)}\|$ since for all k the norm is the same.

$$\begin{aligned}
\mathbb{E}_X \left[\|X^T w^* - X^T (w^* \odot m)\|^2 \right] &\stackrel{\text{Lemma 4.3}}{=} \mathbb{E}_X \left[\frac{1}{s} \sum_{k=1}^d \frac{\sum_{j=1}^d \|X_{(j)}\| |w_j^0|}{|w_k^0|} \|X_{(k)}\| w_k^{*2} \right] \\
&= \frac{1}{s} \sum_{k=1}^d w_k^{*2} \left(\mathbb{E}_X \left[\|X_{(k)}\|^2 \right] + \frac{1}{|w_k^0|} \sum_{j \neq k} |w_j^0| \mathbb{E}_X \left[\|X_{(k)}\| \right] \mathbb{E}_X \left[\|X_{(j)}\| \right] \right) \\
&= \frac{1}{s} \sum_{k=1}^d \mathbb{E}_X \left[\|X_{(\cdot)}\|^2 \right] w_k^{*2} + \mathbb{E}_X \left[\|X_{(\cdot)}\| \right]^2 \frac{w_k^{*2}}{|w_k^0|} \sum_{j \neq k} |w_j^0|
\end{aligned}$$

Note that according to X distribution,

$$\begin{aligned}
\mathbb{E}_X \left[\|X_{(\cdot)}\|^2 \right] &= \mathbb{E} \left[\sum_{i=1}^n \frac{1}{n} x_i^2 \right] = 1, \\
\mathbb{E}_X \left[\|X_{(\cdot)}\| \right]^2 &= \frac{1}{n} \mathbb{E} \left[\sqrt{\sum_{i=1}^n x_i^2} \right]^2 = \frac{2}{n} \frac{\Gamma((n+1)/2)^2}{\Gamma(n/2)^2} \leq 1.
\end{aligned}$$

Where $\Gamma(\cdot)$ is the gamma function.

Calculate the result as a function of $\|w^* - w^0\|$:

$$\begin{aligned}
\frac{1}{s} \sum_{k=1}^d w_k^{*2} + \frac{w_k^{*2}}{|w_k^0|} \sum_{j \neq k} |w_j^0| &= \frac{1}{s} \sum_{k=1}^d \frac{w_k^{*2}}{|w_k^0|} \sum_{j=1}^d |w_j^0| \\
&= \frac{1}{s} \|w^0\|_1 \sum_{k=1}^d \frac{w_k^*}{|w_k^0|} \\
&= \frac{1}{s} \|w^0\|_1 \sum_{k=1}^d \frac{(w_k^* - w_k^0)^2}{|w_k^0|} + 2 \text{sign}(w_k^0) w_k^* - |w_k^0| \\
&\leq \frac{1}{s} \|w^0\|_1 \left(\frac{\|w^* - w^0\|_2^2}{\|w^0\|_\infty} + 2\|w^*\|_1 - \|w^0\|_1 \right) \\
&\leq \frac{1}{s} \|w^0\|_1 \left(\frac{\|w^* - w^0\|_2^2}{\|w^0\|_\infty} + 2\|w^* - w^0\|_1 + \|w^0\|_1 \right)
\end{aligned}$$

Where the last inequality holds from the reverse triangle inequality and addition and subtraction of $\|w^0\|_1$. \square

B.5 Proof of Lemma 4.5

Lemma 4.5. *Suppose $X \in \mathbb{R}^{d \times n} \sim \frac{1}{\sqrt{n}} \mathcal{N}(0, I)$, $w^0 \in \mathbb{R}^d$ and $s \in \mathbb{Z}^+$, then when choosing m uniformly at random the error can be bounded*

$$\begin{aligned}
&\mathbb{E}_X \left[\|X^T w^* - X^T (w^* \odot m)\|^2 \right] \\
&\leq \frac{d}{s} \|w^*\|^2 = \frac{d}{s} \left(\|w^* - w^0\|^2 + 2w^{*T} w^0 \right) - \frac{d}{s} \|w^0\|^2.
\end{aligned}$$

Proof. This proof is in the same form as Theorem 4.4 and we start by establishing the equivalence to Lemmas B.1 and B.2. In order to maintain the estimation of the features, when $m_i \neq 0$ it holds that $m_i = \frac{d}{s}$ (as stated in Algorithm 1, $m_i = \frac{1}{sp_i}$).

$$\mathbb{E}_m \left[(X^T (w^* \odot m))_i \right] = \sum_{t=1}^s \frac{1}{d} (X^T w^*)_i \frac{d}{s} = (X^T w^*)_i$$

Next we analyse the variance $\text{Var}_m \left[(X^T (w^* \odot m))_i \right]$. Fix an index i and let $Y_t^{Unis^*} = \frac{X_{it} w_{it}^*}{sp_{it}^{Unis^*}} = \frac{dX_{it} w_{it}^*}{s}$. We look at

$$\begin{aligned}
\text{Var} \left[(X^T (w^* \odot m))_i \right] &= \sum_{t=1}^s \text{Var} \left[Y_t^{Unis^*} \right] = \sum_{t=1}^s \mathbb{E} \left[(Y_t^{Unis^*})^2 \right] - \mathbb{E} \left[Y_t^{Unis^*} \right]^2. \\
\mathbb{E}_m \left[Y_t^{Unis^*2} \right] &= \sum_{k=1}^d \frac{X_{ki}^2 (w_k^*)^2}{s} \frac{d}{s}
\end{aligned}$$

Overall we can conclude that

$$\text{Var}_m \left[(X^T (w^* \odot m))_i \right] = \frac{d}{s} \sum_{k=1}^d X_{ki}^2 (w_k^*)^2 - \frac{1}{s} (X^T w^*)_i^2.$$

Finally we calculate the expectation over X and we have

$$\mathbb{E}_{X,m} \left[\|X^T w^* - X^T (w^* \odot m)\| \right] \leq \frac{d}{s} \|w^*\|^2 = \frac{d}{s} \left(\|w^* - w^0\|^2 + 2w^{*T} w^0 \right) - \frac{d}{s} \|w^0\|^2$$

\square

B.6 Proof of Theorem 7.2

Theorem 7.2. *Under [1-4] assumptions, $\delta_0 > 0$ and $\eta_0 \leq \eta_{critical}$. Let $m \in \mathbb{R}^d$ be a s -dense mask found with Algorithm 1 with p according to $f_0^{lin}(\mathcal{X})$ and θ_0 (Equation (2)). Then there exist $R_0 > 0$, $K > 1$ such that for every $n \geq N$ the following holds with probability $> 1 - \delta_0$ over random initialization when applying GD with η_0*

$$\begin{aligned} & \mathbb{E}_m \left[\|f_t^{lin}(\mathcal{X}) - \nabla_{\theta_t} f_t(\mathcal{X})(\theta_t \odot m)\|^2 \right] \\ & \leq \frac{1}{s} K^3 \|\theta_0\|_1 F(J(\theta_0)) \cdot \\ & \quad \left(\|\theta_0\|_1 + F(\theta_0) \frac{9K^4 R_0^2}{\lambda_{\min}^2} + 6\sqrt{d} \frac{K^3 R_0}{\lambda_{\min}} \right), \end{aligned}$$

where $F(A) = \sum_{i=1}^d \frac{1}{\|A^{(i)}\|}$.

Proof. We start with computing the expected error of approximation of the features at time t using Lemma 4.3. Note that we use the jacobian at initialization $J(\theta_0)$ and the initial parameters θ_0 to find the mask m .

$$\begin{aligned} \mathbb{E}_m \left[\|f_t^{lin}(\mathcal{X}) - \nabla_{\theta_t} f_t(\mathcal{X})(\theta_t \odot m)\| \right] &= \mathbb{E}_m \left[\|J(\theta_t)\theta_t - J(\theta_t)(\theta_t \odot m)\|^2 \right] \\ &\leq \frac{1}{s} \sum_{k=1}^d \frac{\|J(\theta_t)^{(k)}\|^2}{\|J(\theta_0)^{(k)}\|} \frac{\theta_{tk}^2}{|\theta_{0k}|} \sum_{j=1}^d \|J(\theta_0)^{(j)}\| \|\theta_{0j}\| \\ &\leq \frac{1}{s} \left(\sum_{j=1}^d \|J(\theta_0)^{(j)}\| \|\theta_{0j}\| \right) \left(\sum_{k=1}^d \frac{\|J(\theta_t)^{(k)}\|^2}{\|J(\theta_0)^{(k)}\|} \right) \left(\sum_{k=1}^d \frac{\theta_{tk}^2}{|\theta_{0k}|} \right) \end{aligned}$$

Next we bound each term.

$$\begin{aligned} \sum_{k=1}^d \frac{\theta_{tk}^2}{|\theta_{0k}|} &= \sum_{k=1}^d \frac{(\theta_{tk} - \theta_{0k})^2}{|\theta_{0k}|} + 2\theta_{tk} \text{sign}(\theta_{0k}) - |\theta_{0k}| \\ &\leq \left(\sum_{k=1}^d \frac{1}{|\theta_{0k}|} \right) \|\theta_t - \theta_0\|^2 + 2\|\theta_t\|_1 - \|\theta_0\|_1 \\ &\leq \left(\sum_{k=1}^d \frac{1}{|\theta_{0k}|} \right) \|\theta_t - \theta_0\|^2 + 2\|\theta_t - \theta_0\|_1 + \|\theta_0\|_1 \end{aligned}$$

Where the last transition is done we the reverse triangle inequality and subtraction and addition of $\|\theta_0\|_1$. Hence when using the bound in Theorem G.4 and $\|a\|_1 \leq \sqrt{d}\|a\|_2$ we have,

$$\sum_{k=1}^d \frac{\theta_{tk}^2}{|\theta_{0k}|} \leq \|\theta_0\|_1 + \left(\sum_{k=1}^d \frac{1}{|\theta_{0k}|} \right) \left(\frac{3KR_0}{\lambda_{\min}} \right)^2 + 6\sqrt{d} \frac{KR_0}{\lambda_{\min}}$$

We bound the next term,

$$\begin{aligned} & \left(\sum_{j=1}^d \|J(\theta_0)^{(j)}\| \|\theta_{0j}\| \right) \left(\sum_{k=1}^d \frac{\|J(\theta_t)^{(k)}\|^2}{\|J(\theta_0)^{(k)}\|} \right) \leq \left(\sum_{j=1}^d \|J(\theta_0)^{(j)}\| \|\theta_{0j}\| \right) \left(\sum_{k=1}^d \frac{1}{\|J(\theta_0)^{(k)}\|} \right) \left(\sum_{k=1}^d \|J(\theta_t)^{(k)}\|^2 \right) \\ & = \left(\sum_{j=1}^d \|J(\theta_0)^{(j)}\| \|\theta_{0j}\| \right) \left(\sum_{k=1}^d \frac{1}{\|J(\theta_0)^{(k)}\|} \right) \|J(\theta_t)\|_F^2 \\ & \leq \left(\sum_{j=1}^d \|J(\theta_0)^{(j)}\| \|\theta_{0j}\| \right) \left(\sum_{k=1}^d \frac{1}{\|J(\theta_0)^{(k)}\|} \right) K^2 \end{aligned}$$

We can also bound,

$$\left(\sum_{j=1}^d \|J(\theta_0)^{(j)}\| |\theta_{0j}| \right) \leq \sum_{j=1}^d \|J(\theta_0)\|_F |\theta_{0j}| \leq K \|\theta_0\|_1$$

Overall we can bound the error with the state of the model at initialization

$$\begin{aligned} \mathbb{E}_m \left[\|J(\theta_t)\theta_t - J(\theta_t)(\theta_t \odot m)\|^2 \right] &\leq \\ &\leq \frac{1}{s} K^3 \|\theta_0\|_1 \left(\sum_{k=1}^d \frac{1}{\|J(\theta_0)^{(k)}\|} \right) \left(\|\theta_0\|_1 + \left(\sum_{k=1}^d \frac{1}{|\theta_{0k}|} \right) \left(\frac{3K^2 R_0}{\lambda_{\min}} \right)^2 + 6\sqrt{d} \frac{K^3 R_0}{\lambda_{\min}} \right) \\ &\leq \frac{1}{s} K^3 \|\theta_0\|_1 F(J(\theta_0)) \left(\|\theta_0\|_1 + F(\theta_0) \frac{9K^4 R_0^2}{\lambda_{\min}^2} + 6\sqrt{d} \frac{K^3 R_0}{\lambda_{\min}} \right) \end{aligned}$$

Where $F(A) = \sum_{i=1}^d \frac{1}{\|A^{(i)}\|}$.

□